SUPPLEMENTARY APPENDIX

CDCA7 finely tunes cytoskeleton dynamics to promote lymphoma migration and invasion

Carla Martín-Cortázar,[1] Yuri Chiodo,[1] Raul Jiménez-P.,[1] Manuel Bernabé,[2] María Luisa Cayuela,[2] Teresa Iglesias[3,4] and Miguel R. Campanero[1,5]

[1]Department of Cancer Biology, Instituto de Investigaciones Biomédicas Alberto Sols, Madrid; [2]Telomerase, Aging and Cancer Group, Research Unit, Department of Surgery, CIBERehd, Instituto Murciano de Investigación Biosanitaria (IMIB), Murcia; [3]Department of Endocrine and Nervous Systems Pathophysiology, Instituto de Investigaciones Biomédicas Alberto Sols, Madrid ; [4]Centro de Investigación Biomédica en Red de Enfermedades Neurodegenerativas (CIBERNED), Madrid and [5]Centro de Investigaciones Biomédicas en Red en Enfermedades Cardiovasculares (CIBERCV), Madrid, Spain

 doi:10.3324/haematol.2018.215459

Received: December 31, 2018.

Accepted: June 19, 2019.

Pre-published: June 20, 2019.

Correspondence: *MIGUEL R. CAMPANERO* - mcampanero@iib.uam.es

CDCA7 finely tunes cytoskeleton dynamics to promote lymphoma migration and invasion

Carla Martín-Cortázar[1], Yuri Chiodo[1], Raúl Jiménez-P.[1], Manuel Bernabé[2], María Luisa Cayuela[2], Teresa Iglesias[3,4], and Miguel R. Campanero[1,5].

SUPPLEMENTARY DATA

Supplementary Methods

Cell lines

Human Burkitt lymphoma cell lines DG-75 (CRL-2625) and BL-2 (ACC-625), and Diffuse Large B-Cell lymphoma cell line Toledo (CRL-2631) were obtained from ATCC (LGC Standards S.L.U., Barcelona, Spain) and cultured in RPMI 1640 medium (21875-034) supplemented with 10% fetal bovine serum (FBS; 1027106) and 2 mM glutamine (25030-081), all from ThermoFisher Scientific (Waltham, MA, USA), plus 100 units/ml penicillin (Laboratorios ERN.S.A., Madrid, Spain; 804443) and 100 µg/ml streptomycin (Reig Jofre S.A., Madrid, Spain; 753483) and were maintained at 37°C in a humidified incubator with 5% CO_2.

Lentivirus production and cell transduction.

Lentiviral particles were produced as previously described (1) employing MISSION pLKO.1-puro-based vectors (Sigma-Aldrich, Madrid, Spain,) encoding either a non-targeting shRNA (SHC002) or *CDCA7*-targeting shRNAs sh-25 (TRCN0000140725) and sh-83 (TRCN0000145183). Conditioned medium was harvested and filtered through 0.45-µm filters. DG-75, BL-2, and Toledo cell lines were incubated with viral particles in culture medium with 8µg/ml protamine sulfate during 16 h. Cells were washed to remove viral particles and

transduced cells were selected in the presence of 1μg/ml puromycin (Sigma-Aldrich, P8833) for at least 96 h.

Antibodies

Antibodies to α-tubulin (T9026), α-actinin (monoclonal; A5044) and α-actinin (polyclonal; A2543) were obtained from Sigma-Aldrich. Anti-pMLC and anti-TPM3 were from Cell Signaling technology (#3675) and Biorbyt (orb192140), respectively. The anti-CDCA7 S99 polyclonal rabbit serum was reported before (2). A non-specific monoclonal antibody (X63) and mAbs to CD45 (D3/9), MHC class I (W6/32), β1 integrin subunit (TS2/16), active β1 integrin subunit (HUTS-21), α4 integrin subunit (HP2/1) and α5 integrin subunit (P1D6), were kindly provided by Dr. Francisco Sánchez-Madrid (Hospital La Princesa, Madrid, Spain) as hybridoma culture supernatants. Purified mouse anti-human CD184 was acquired from Becton Dickinson Biosciences (San Jose, CA, USA; 555972).

Donkey anti-rabbit IgG, goat anti-mouse IgG, and goat anti-mouse IgG conjugated to IR-800Dye (926-32213), IR-800Dye (926-32210), and IR680Dye (926-32220), respectively were purchased from LI-COR Biosciences (Lincoln, Nebraska, USA). Goat anti-rabbit IgG conjugated to Alexa fluor 488 (A-11034) or Alexa fluor 647 (A-21245), and goat anti-mouse IgG conjugated to Alexa fluor 488 (A-11029) or Alexa fluor 546 (A-11030), were obtained from ThermoFisher Scientific.

Western Blotting

Cells were harvested and suspended in Total Lysis Buffer (0.125 M Tris-HCl pH 6.8, 4% SDS and 20% glycerol). Cell lysates were boiled for 15 min and protein concentration was determined by the Lowry method. After quantification, β-mercaptoethanol (1:100 v/v) and bromophenol blue powder were added. Protein samples were resolved in 8% SDS-PAGE and transferred to nitrocellulose membranes as described (3). Membranes were probed with anti-CDCA7 S99 (1:5,000), anti-α-tubulin (1:40,000), or anti-α-actinin (1:500), followed by the

corresponding IR-dye-conjugated secondary antibody (1:15,000), and scanned using an Odyssey® Infrared imaging system (Model 9120, LI-COR Biosciences).

Xenografts

DG-75 cells ($2x10^6$) in 0.1 ml of phosphate buffer saline (PBS) were injected subcutaneously in the dorsal flanks of 8- to 10-week-old NOD-SCID mice. Tumor masses were extracted after 3 weeks, fixed with 4% formaldehyde in PBS, and embedded in paraffin. Paraffin-embedded tissue samples were stained with hematoxylin, as previously described (4). The specimens were analyzed by microscopy, using an Eclipse 90i Nikon microscope (Nikon Instruments Europe, Amsterdam, Netherlands). Images were taken with a DS-Fi1 camera (Nikon). All animal procedures were approved by the CSIC Ethics Committee (ref. 054/2014 and 634/2017) and by the Madrid Regional authorities (ref. PROEX 31/14 and 215/17), and conformed to EU Directive 2010/63EU and Recommendation 2007/526/EC regarding the protection of animals used for experimental and other scientific purposes, enforced in Spanish law under Real Decreto 1201/2005. Overall mouse health was assessed by daily inspection for signs of discomfort, weight loss, or changes in behaviour, mobility, and feeding or drinking habits.

***In vitro* migration and invasion assays**

Transwell migration and invasion assays were carried out in Boyden chambers using filters (3-µm pore size; Corning Incorporated, New York; #3415). Filters were coated with 20 µg/ml fibronectin (Sigma-Aldrich, F1056) or with a 10% matrigel (Becton Dickinson Biosciences; 356231) solution in RPMI for migration and invasion assays, respectively. Cells ($5x10^5$) were washed twice with RPMI; suspended in 100 µl of this medium, supplemented, when appropriate, with 0.1 µg/ml cytochalasin D (Sigma-Aldrich; C8273), 20 µM fasudil (Selleckchem, Houston, Texas, S1573) or 25 µM blebbistatin (Selleckchem; S7099); and seeded in the upper chamber of coated transwells. RPMI medium (600 µl) was added to the lower chamber supplemented with 10% FBS or 50 ng/ml SDF1 (PeproTech, London, UK; 300-

28A) as chemotactic stimuli. Transwells were maintained during 24 h (migration) or 48 h (invasion) at 5% CO_2 and 95% humidity. Cells were then recovered from the lower chamber and counted in the presence of trypan blue (Sigma-Aldrich, T8154) using a hemocytometer. Experiments were performed in duplicate and repeated at least three times.

Zebrafish invasion assays

The adult fish were maintained at 28°C in aquaria with 14 hours of day and 10 hours of night cycles. Embryos were kept in E3 medium at 28°C until they reached the desired embryonic stage. Transduced DG-75 or Toledo cells ($2x10^6$) were stained with 10 µg/ml Cell Tracker CM-DiI dye (Life Technologies, C7001) and then transferred into the yolk sac of 30-50 zebrafish embryos (100-150 cells per embryo) at 48 h post fertilization. The amount of injected cells was similar for all cell groups and showed only a slight variation between the embryos. Embryos were incubated at 28.5ºC for 48 hours before imaging (SteReo Lumar V12 stereomicroscope equipped with an AxioCam MR5 camera (Carl Zeiss)) and scoring the position of the transplanted cells. Invasion capacity was determined as the percentage of embryos showing >5 cells outside the yolk sac. At least 30 embryos were injected with each cell group, and experiments were performed 4 times minimum for all cell groups. The experiments performed comply with the Guidelines of the European Union Council (Directive 2010/63/EU) and the Spanish RD 53/2013.

Quantitative PCR (qPCR)

Total RNA was extracted from exponentially-growing DG-75, BL-2, Toledo, MCF-7, and SW480 cells, using TRIzol reagent (ThermoFisher Scientific; 15596026). The Genomic Facility at Instituto de Investigaciones Biomedicas synthesized complementary DNA using M-MLV retro transcriptase (ThermoFisher Scientific) and analyzed gene expression by real-time quantitative RT–PCR (qPCR) using TaqMan Gene Expression Assays (ThermoFisher Scientific) specific for *CDCA-7* (Hs00230589_m1), *MMP2* (Hs01548727_m1), *MMP9* (Hs00234579_m1), and *EZH2* (Hs00544830_m1). *ACTB* (Hs99999903_m1) was used as a

control gene on the basis of its homogeneous expression in used cell lines. Calculations were made from measurements of 3 replicates of each sample.

Flow cytometry

Cells ($5x10^5$) were incubated for 30 min at 4°C with hybridoma culture supernatant (100 µl) or purified anti-CD184 (1 µg), washed twice with PBS and then incubated with Alexa fluor 488-conjugated goat anti-mouse IgG (A-11029) (100 µl). Flow cytometry analysis was performed on a FACScan cytofluorometer (Becton Dickinson).

Adhesion assays

For cell adhesion assays, 100 µl/well of 20µg/ml fibronectin (Sigma-Aldrich; F1056) were used to coat 96-well high-binding plates (Corning Incorporated; #3590) for 18 h at 4ºC. Plates were then saturated with PBS containing 0.5% denatured bovine serum albumin (BSA; Sigma-Aldrich; 10735086001) for 30 min at 37ºC and washed with PBS. Cells (10^5 per well in 100 µl of RPMI) were added and the plates were centrifuged at 10 x g before incubation at 37ºC for 45 min. SDF1 (10 ng/ml) or 10 µl crude TS2/16 hybridoma culture supernatant were added before centrifugation. The TS2/16 antibody increases the avidity and the affinity of ß1 integrins for their substrates (5). Plates were washed with RPMI and images of the wells were acquired with a Nikon 90i microscope using a 4x Plan-apo objective (Nikon) and processed with NisElements 3.01 (Nikon) and ImageJ 1.48v (NIH) software to determine the number of cells per well. Total cellular input was calculated by spinning wells with original number of cell aliquots.

Immunofluorescence

For immunofluorescence staining, cells (10^5 cells in 100 µl of RPMI) were incubated on coverglasses previously coated with 2 µg fibronectin (18 h at 4ºC) and then treated at 37ºC for 15 min with 10 ng/ml SDF1. Cells were fixed with 4% formaldehyde plus 4% sucrose in PBS (15 min at room temperature (RT)), permeabilized with 0.1% Triton X-100 in PBS (5 min at RT), and treated with blocking solution (5% goat serum plus 5% BSA in PBS) 30 min at RT.

Coverslips were then incubated for 1 h at RT with anti-α-tubulin (1:2,000), anti-α-TPM3 (1:500), anti-pMLC (1:500), anti-α-actinin monoclonal or polyclonal (1:250), or HUTS-21 (100 µl hybridoma culture supernatant), followed by the corresponding secondary antibody (1:500). The non-specific mouse monoclonal antibody X63 (100 µl hybridoma culture supernatant) and a non-immune rabbit serum (1:250), followed by the corresponding secondary antibody, were used as negative control. Images of representative staining with these negative control antibodies are shown in Supplementary Figure 10. Filamentous actin and nuclei were stained with phalloidin conjugated to Alexa fluor 546 (1:100; ThermoFisher Scientific; A22283) and DAPI (1:500; ThermoFisher Scientific; D1306), respectively. Coverslips were mounted with ProLong medium (ThermoFisher Scientific; P36930). Confocal microscopy images were acquired in an inverted Zeiss LSM710 laser-scanning microscope using a 63x Plan-apochromat objective (Zeiss, Germany) and 2x zoom. Sequential scanning mode was used to avoid crosstalk between channels. Images were processed with Zen 2009 (Carl Zeiss MicroImaging), Adobe Photoshop CS (Adobe Systems Inc.) and ImageJ 1.52b software (NIH).

Fluorescence intensity was quantified by thresholding the color signal using the hue-saturation-intensity color model, determining the percentage of stained area, and normalizing with the number of cells in each image. To determine cell-staining polarization, cells were splitted, after thresholding the color signal, in 8 equal sections using the ImageJ “Draw circles and quadrants” tool (https://gist.github.com/lacan/8acb3bfe51eb1b1ba6c60fba75e085a8). A cell was considered as polarized when no staining was detected in >2 contiguous sections. The total number of cells and the number of polarized cells were then quantified with ImageJ. Colocalization of fluorescent signals was analyzed using the ImageJ “JACoP (Just Another Colocalization Plugin)” plugin. Pearson’s and Mander’s coefficients were used to determine the relative correlation and relative overlapping of signals, respectively. All analyses were performed using at least three independent images from each of three independent experiments, and included >60 cells per image.

Statistical analysis

GraphPad Prism software 6.01 was used for the analysis. Differences were analyzed by one-way analysis of variance (ANOVA) with Bonferroni post-test, one-tailed t-test, or Chi-square with two-tailed Fisher's exact test, as appropriate. Differences were considered significant at $p<0.05$.

The numbers of animals used are described in the corresponding figure legends. All experiments were carried out with at least three biological replicates. Experimental groups were balanced in terms of animal age and weight. Animals were caged together and treated in the same way. Appropriate tests were chosen according to the data distribution. Variance was comparable between groups throughout the manuscript. No randomization was used to allocate animals to experimental groups and investigators were not blinded to the group allocation during experiments or outcome assessments.

REFERENCES

1. Alvaro-Blanco J, Urso K, Chiodo Y, et al. MAZ induces MYB expression during the exit from quiescence via the E2F site in the MYB promoter. Nucleic Acids Res. 2017;45(17):9960-9975.

2. Jimenez PR, Martin-Cortazar C, Kourani O, et al. CDCA7 is a critical mediator of lymphomagenesis that selectively regulates anchorage-independent growth. Haematologica. 2018;103(10):1669-1678.

3. Campanero MR, Herrero A, Calvo V. The histone deacetylase inhibitor trichostatin A induces GADD45 gamma expression via Oct and NF-Y binding sites. Oncogene. 2008;27(9):1263-1272.

4. Molina-Privado I, Jimenez PR, Montes-Moreno S, et al. E2F4 plays a key role in Burkitt lymphoma tumorigenesis. Leukemia. 2012;26(10):2277-2285.

5. Arroyo AG, Garcia-Pardo A, Sanchez-Madrid F. A high affinity conformational state on VLA integrin heterodimers induced by an anti-beta 1 chain monoclonal antibody. J Biol Chem. 1993;268(13):9863-9868.

Supplementary Tables and Figures

Mouse	shRNA	Tumor weight (g)	Non-tumoral tissue	Non-tumoral tissue organization
1	sh-Ctl	1.49	Muscle	Dissociated
1	sh-25	0.29	None	-
2	sh-Ctl	1.42	Muscle	Dissociated
2	sh-25	0.15	None	-
3	sh-Ctl	0.72	Fat	Non-dissociated
3	sh-25	0	None	-
4	sh-Ctl	1.51	Muscle	Dissociated
4	sh-25	0.68	Muscle	Non-dissociated
5	sh-Ctl	1.87	Fat	Dissociated
5	sh-25	0.79	Fat	Non-dissociated
6	sh-Ctl	1.11	Muscle and fat	Dissociated
6	sh-25	0.02	None	-
7	sh-Ctl	0.82	Muscle	Dissociated
7	sh-25	0	None	-
8	sh-Ctl	0.84	Muscle	Dissociated
8	sh-83	0.25	Muscle	Non-dissociated
9	sh-Ctl	2.98	Muscle and fat	Dissociated
9	sh-83	0.97	None	-
10	sh-Ctl	0.88	Muscle	Dissociated
10	sh-83	0.02	None	-
11	sh-Ctl	0.73	Muscle	Dissociated
11	sh-83	0.44	Fat	Dissociated
12	sh-Ctl	1.16	Muscle	Non-dissociated
12	sh-83	0	None	-
13	sh-Ctl	1.25	Fat	Dissociated
13	sh-83	0.61	Fat	Non-dissociated

Supplementary Table 1. *CDCA7* silencing limits lymphoma growth and dissociation of neighbor tissues. DG-75 cells were transduced with lentivirus encoding sh-Ctl or the *CDCA7*-specific shRNAs sh-25 and sh-83, selected in the presence of puromycin >5 days, and inoculated subcutaneously in immunodeficient NOD-SCID mice. All mice were inoculated with control cells in one flank and *CDCA7*-silenced cells in the opposite flank, as indicated. Tumors masses grown after 3 weeks were extracted, weighted, and embedded in paraffin. Four non-consecutive tumor sections were stained with hematoxylin and observed under the microscope. The presence of non-tumoral tissue (muscle or fat) and its organization degree (dissociated or non-dissociated) is indicated.

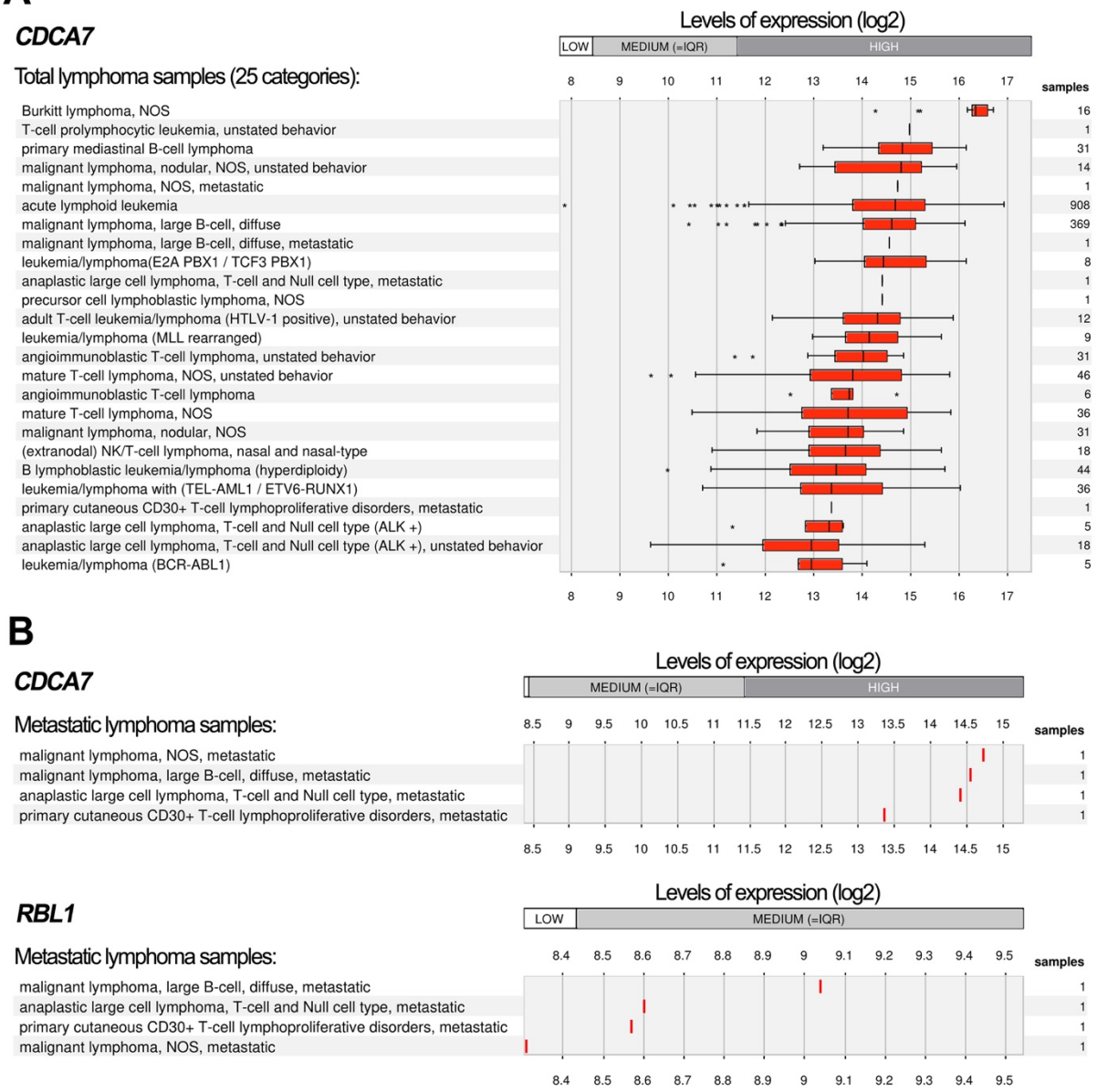

Supplementary Figure 1. *CDCA7* is highly expressed in lymphoid tumor cases. CDCA7 expression was analyzed in gene expression profiles of 1,649 lymphoid tumor cases using the Genevestigator V3 search engine. (**A**) Boxplot representation of *CDCA7* levels (log2) in these cases grouped in 25 categories. NOS, not otherwise specified. The number of samples per category is indicated. Boxes delimit the upper and the lower quartiles, while whiskers represent the lowest and the highest datum within 1.5 of the interquartile range (IQR), and stars represent outliers. LOW, MEDIUM, and HIGH correspond to the first quartile, the IQR, and the fourth quartile expression ranges, considering all expression values of all genes overall samples for the platform in use. (**B**) *CDCA7* levels in the only 4 metastatic lymphoid tumors found in the search engine are indicated by red lines. *RBL1* levels are shown as an example of a gene that is not highly expressed in these cases.

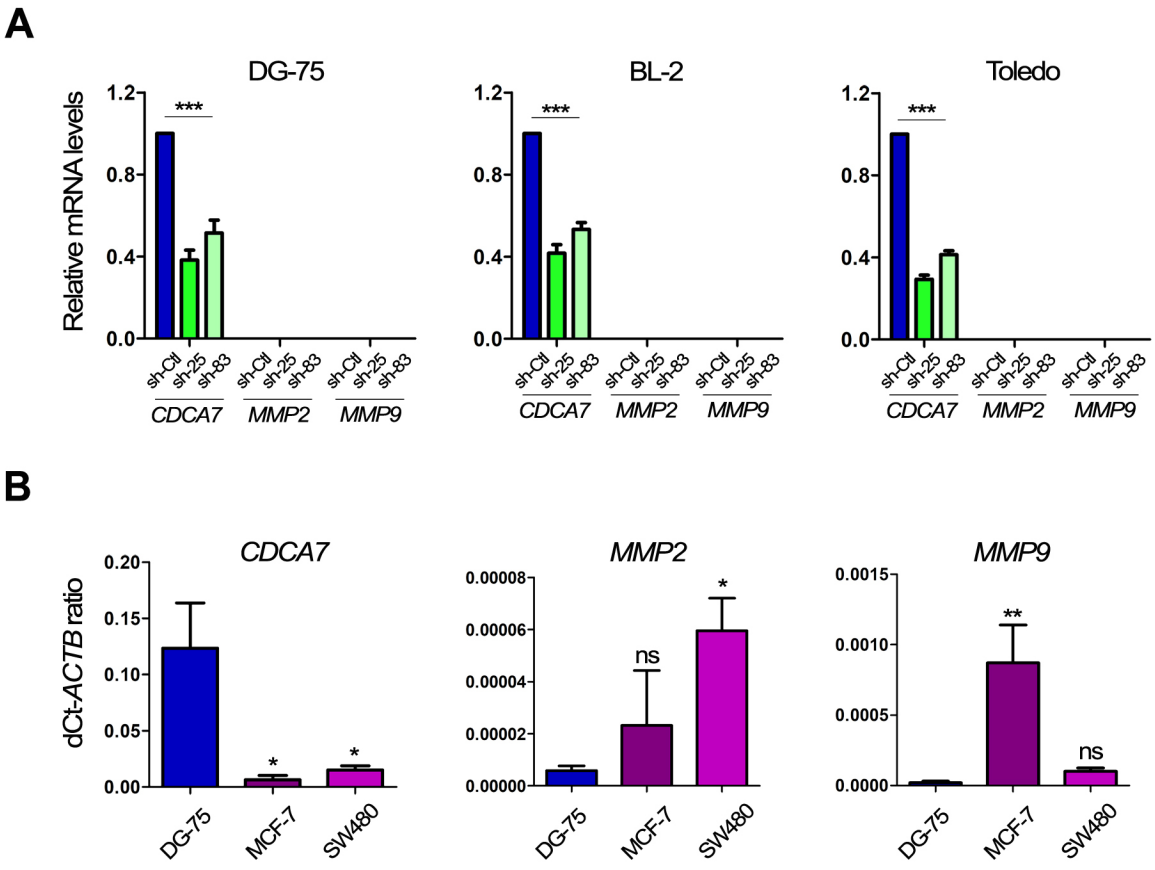

Supplementary Figure 2. *MMP2* and *MMP9* are not expressed in lymphoma cells. qPCR analysis of *CDCA7*, *MMP2, and MMP9* mRNA expression in (**A**) DG-75, BL-2 and Toledo cells transduced with lentivirus encoding the indicated shRNAs and (**B**) MCF-7, SW480, and control-transduced DG-75 cells. (A) Data were normalized to the expression of *ACTB* and are shown relative to control-transduced cells as mean + s.e.m. (n=3). (B) Data are shown relative to *ACTB* expression as mean + s.e.m. (n=3). ns, non-significant; *p<0.05, **p<0.01 and ***p<0.001 (one-way ANOVA with Bonferroni's post-test).

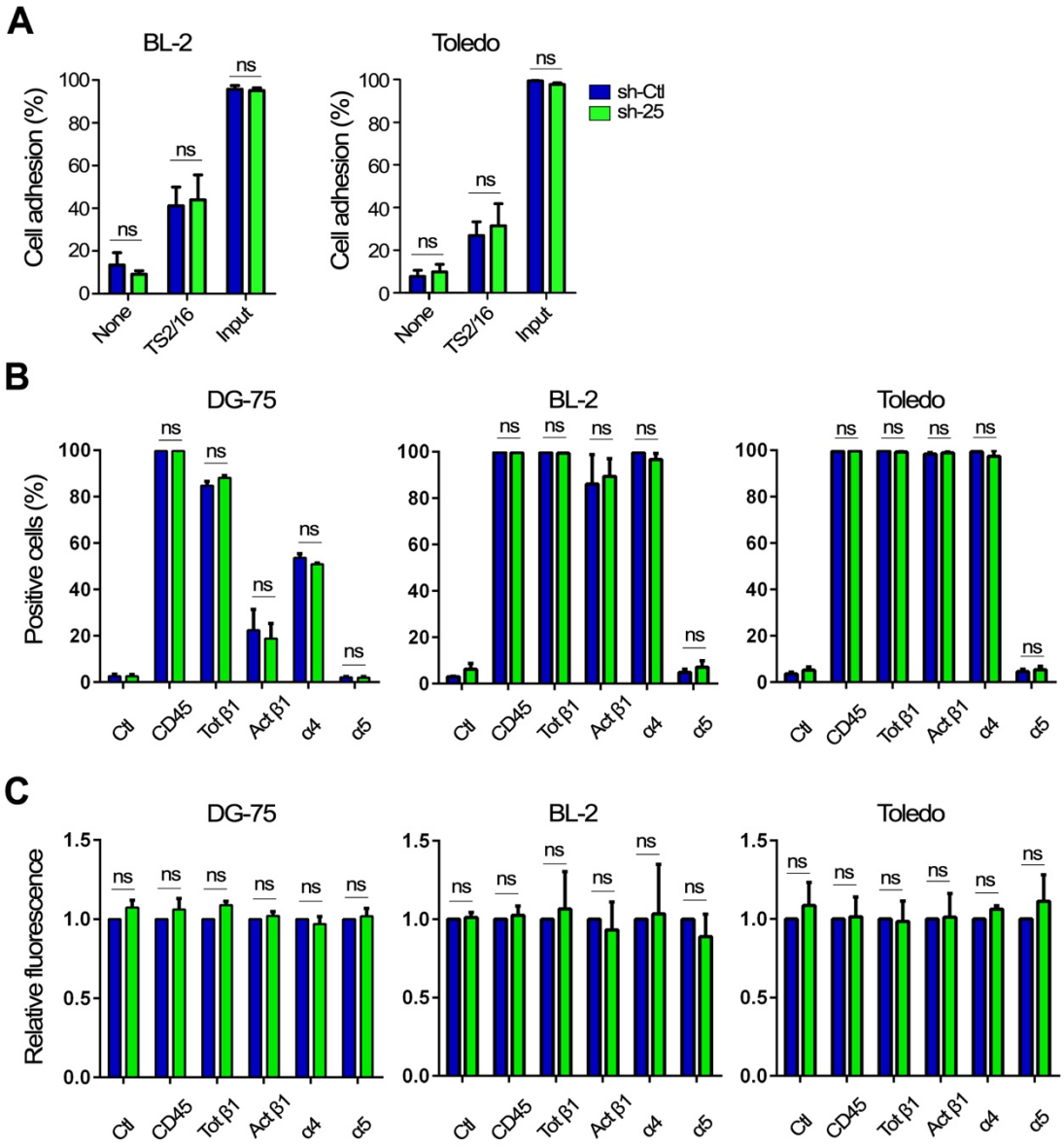

Supplementary Figure 3. *CDCA7* knockdown does not modify cell adhesion to fibronectin or fibronectin receptor levels. (**A**) BL-2 and Toledo cells were transduced with the indicated shRNAs and their relative adhesion to fibronectin was assessed in the absence (None) or the presence of the TS2/16 mAb. The percentage of cells bound to fibronectin and the total cellular input (Input) are shown as mean + s.e.m. of 3 independent transductions. ns, non-significant vs sh-Ctl (One-tailed t-test). (**B-C**) Flow-cytometry analysis of cell surface expression of CD45, total ß1 integrin (Tot ß1), active ß1 integrin (Act ß1), α4 integrin, and α5 integrin in DG-75, BL-2 and Toledo transduced cells. (B) The percentage of positive cells and (C) the relative median fluorescence intensity are shown as mean + s.e.m. of 3 independent lots of transduced cells. ns, non-significant vs sh-Ctl (one-tailed t-test).

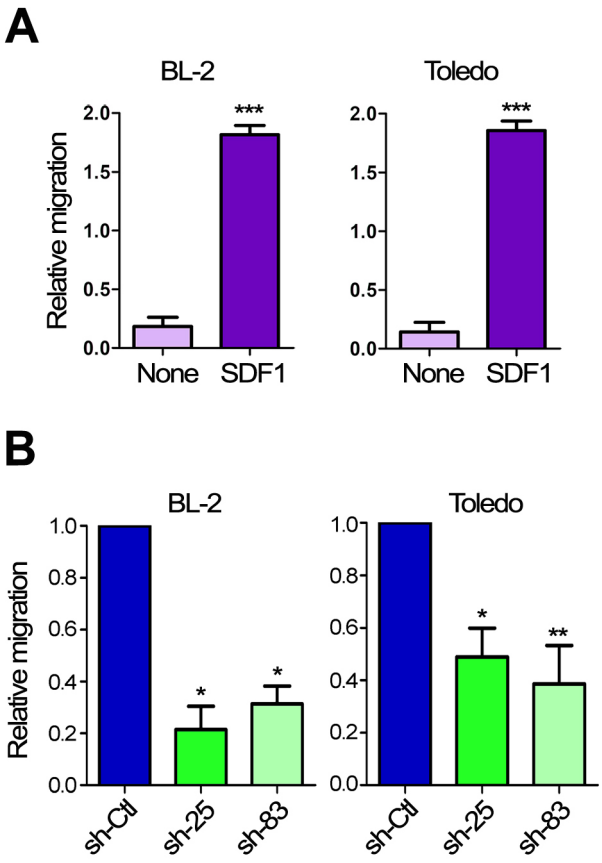

Supplementary Figure 4. *CDCA7* silencing severely disrupts SDF1-induced lymphoma migration. BL-2 and Toledo cells non-transduced or transduced with lentivirus encoding the indicated shRNAs were seeded on the upper surface of the fibronectin-coated polycarbonate membrane of Transwell chambers containing no stimulus (None) or 50 ng/ml SDF1 in the lower chamber. (**A**) Quantification of the relative migration capacity of non-transduced BL-2 and Toledo cells towards SDF1 shown as average + s.e.m. of 3 independent experiments. ***p<0.001 (One-tailed t-test). (**B**) Quantification of the relative SDF1-induced migration of the indicated BL-2 and Toledo transduced cells shown as mean + s.e.m. of 3 independent transductions. *p<0.05, **p<0.01 (one-way ANOVA with Bonferroni's post-test).

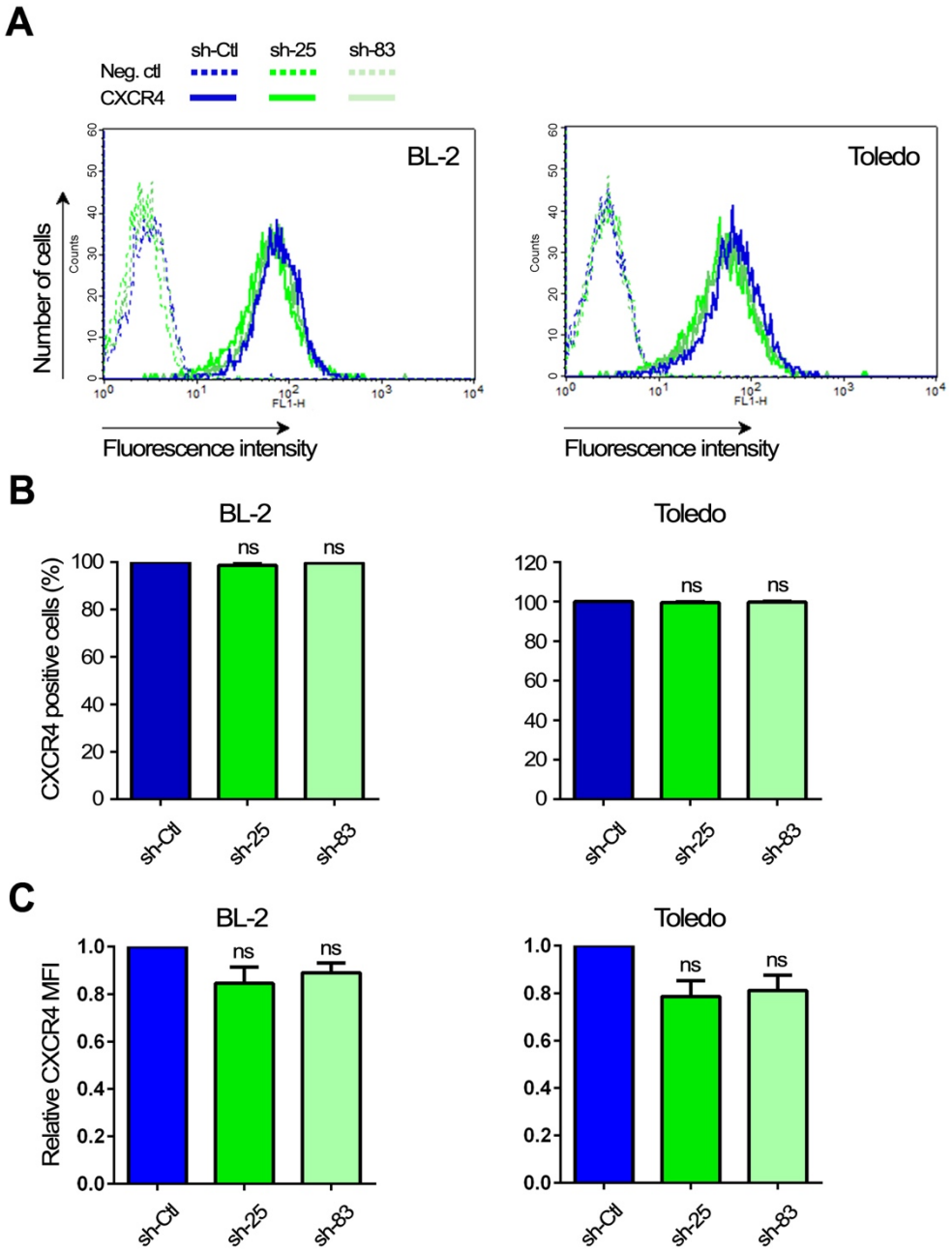

Supplementary Figure 5. *CDCA7* knockdown does not inhibit CXCR4 expression in lymphoma cells. CXCR4 expression was assessed by flow cytometry in BL-2 and Toledo cells transduced with the indicated shRNAs. (**A**) Representative flow cytometry histograms of negative control (dashed lines) and CXCR4 (continuous lines) staining. (**B**) Percentage of CXCR4-positive cells. (**C**) Relative median fluorescence intensity (MFI) of CXCR4 (mean + s.e.m., n=3 independent transductions) in BL-2 and Toledo transduced cells. ns, non-significant vs sh-Ctl (one-way ANOVA with Bonferroni's post-test).

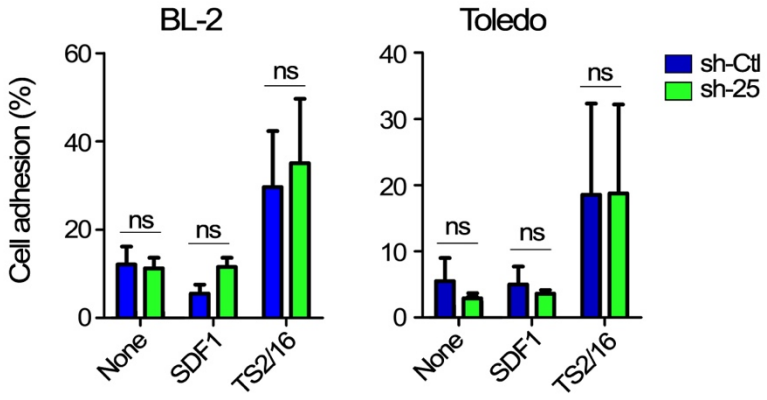

Supplementary Figure 6. *CDCA7* knockdown and SDF1 do not modify lymphoma cell adhesion to fibronectin. BL-2 and Toledo cells were transduced with the indicated shRNAs and their relative adhesion to fibronectin was assessed in untreated cells (None) and in cells treated with SDF1 (10 ng/ml) or the TS2/16 mAb. The percentage of cells bound to fibronectin is shown as mean + s.e.m of 3 independent transductions; ns, non-significant vs sh-Ctl (one-tailed t-test).

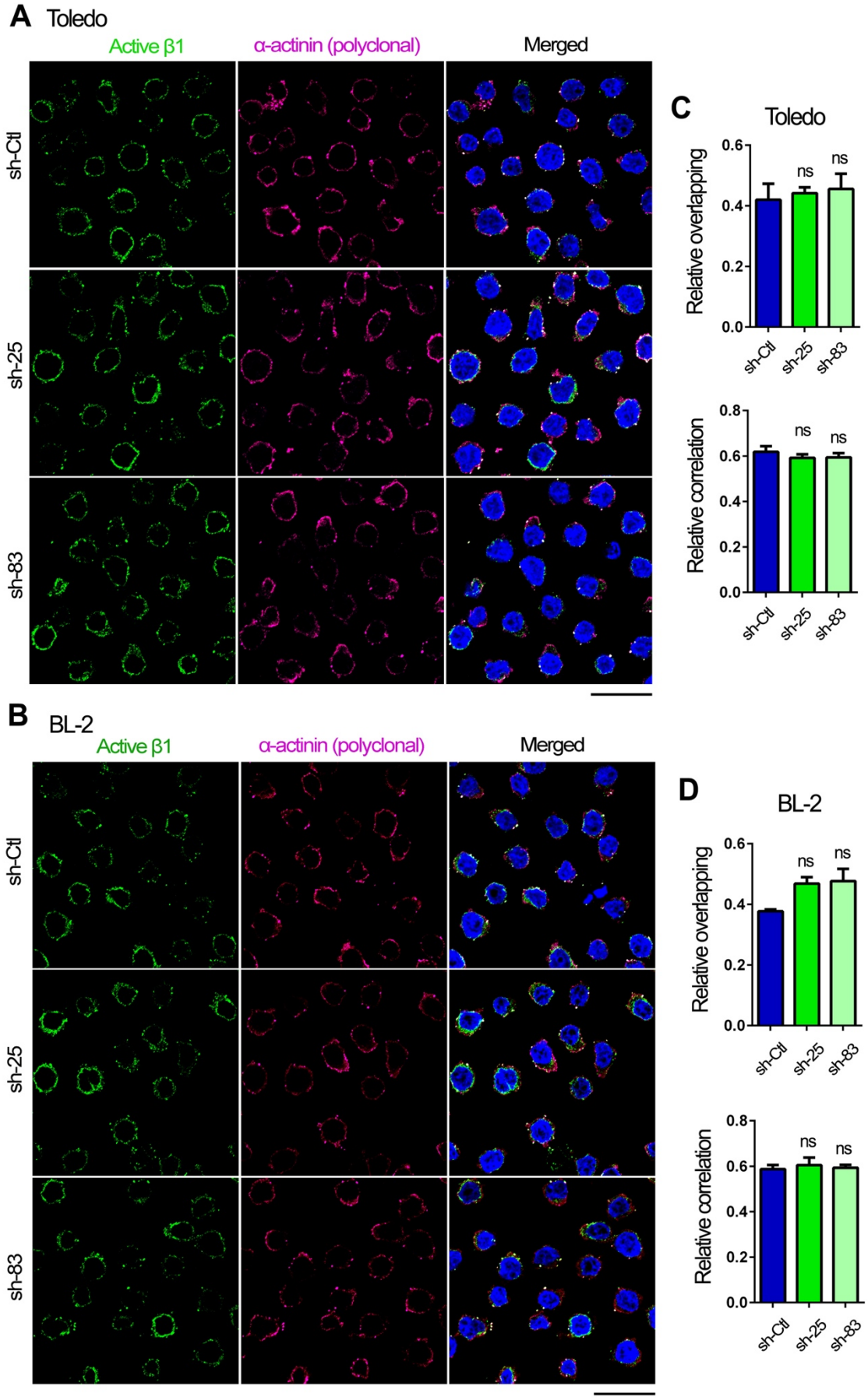

Supplementary Figure 7

Supplementary Figure 7. *CDCA7* silencing does not affect the distribution of α-actinin and active ß1 integrin in lymphoma cells. Toledo and BL-2 cells were transduced with the indicated shRNAs, seeded on coverslips coated with 2 µg fibronectin, and stimulated with 10 ng/ml SDF1 for 15 min. Representative confocal microscopy images (1 section) of transduced (**A**) Toledo and (**B**) BL-2 cells stained with DAPI, a mAb to active integrin ß1, and a polyclonal anti-α-actinin antibody. Scale bar, 10 µm. Quantification of relative α-actinin and active β1 integrin colocalization measured as relative overlapping (Mander's coefficient) and correlation (Pearson's coefficient) of signals in (**C**) Toledo and (**D**) BL2 cells. Data are means + s.e.m. of 3 independent experiments. ns, non-significant (one-way ANOVA with Bonferroni's post-test).

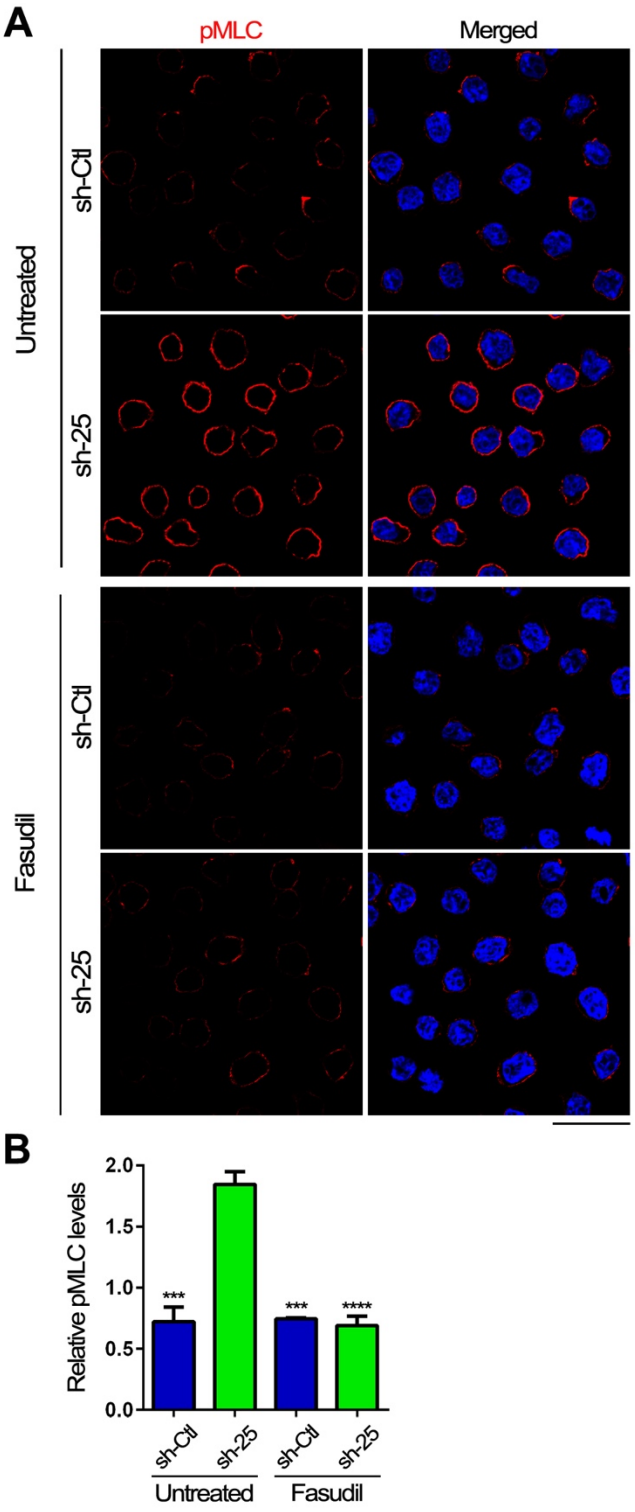

Supplementary Figure 8. The ROCK inhibitor fasudil interferes with MLC phosphorylation. Toledo cells were transduced with the indicated shRNAs, pretreated with 20 µM fasudil for 24h where indicated, seeded on coverslips coated with 2 µg fibronectin, and stimulated with 10 ng/ml SDF1 for 15 min. (**A**) Representative confocal microscopy images (1 section) of these cells stained with anti-phospho-myosin light chain (pMLC) and DAPI. (**B**) Quantification of relative pMLC fluorescence intensity. Data are mean + s.e.m. of 3 independent experiments. ***p<0.001 and ****p<0.0001 (one-way ANOVA with Bonferroni's post-test). Bar, 10 µm.

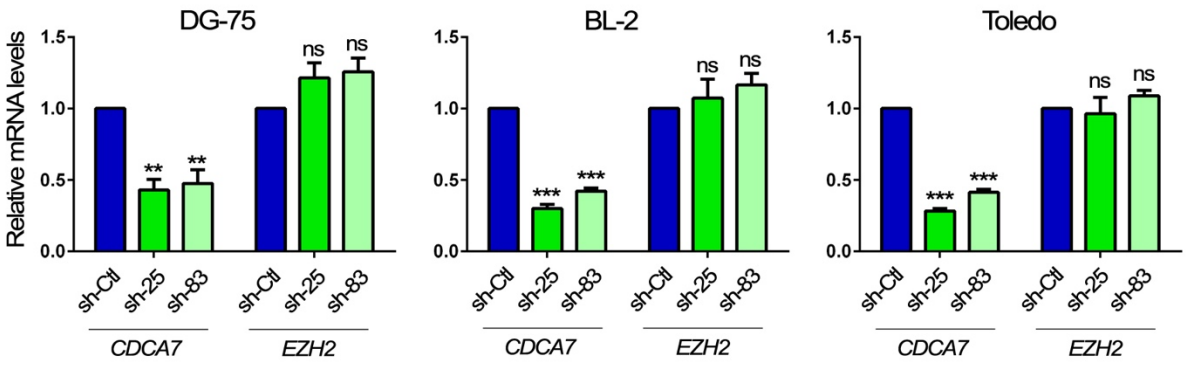

Supplementary Figure 9. CDCA7 silencing does not induce *EZH2* expression in lymphoma cells. qPCR analysis of *CDCA7 and EZH2* mRNA expression in DG-75, BL-2, and Toledo cells transduced with lentivirus encoding the indicated shRNAs. Data were normalized to the expression of *ACTB* and are shown relative to control-transduced cells as mean+s.e.m. (n=3 independent transductions). ns, non-significant vs sh-Ctl; **p<0.01 and ***p<0.001 (one-way ANOVA with Bonferroni's post-test).

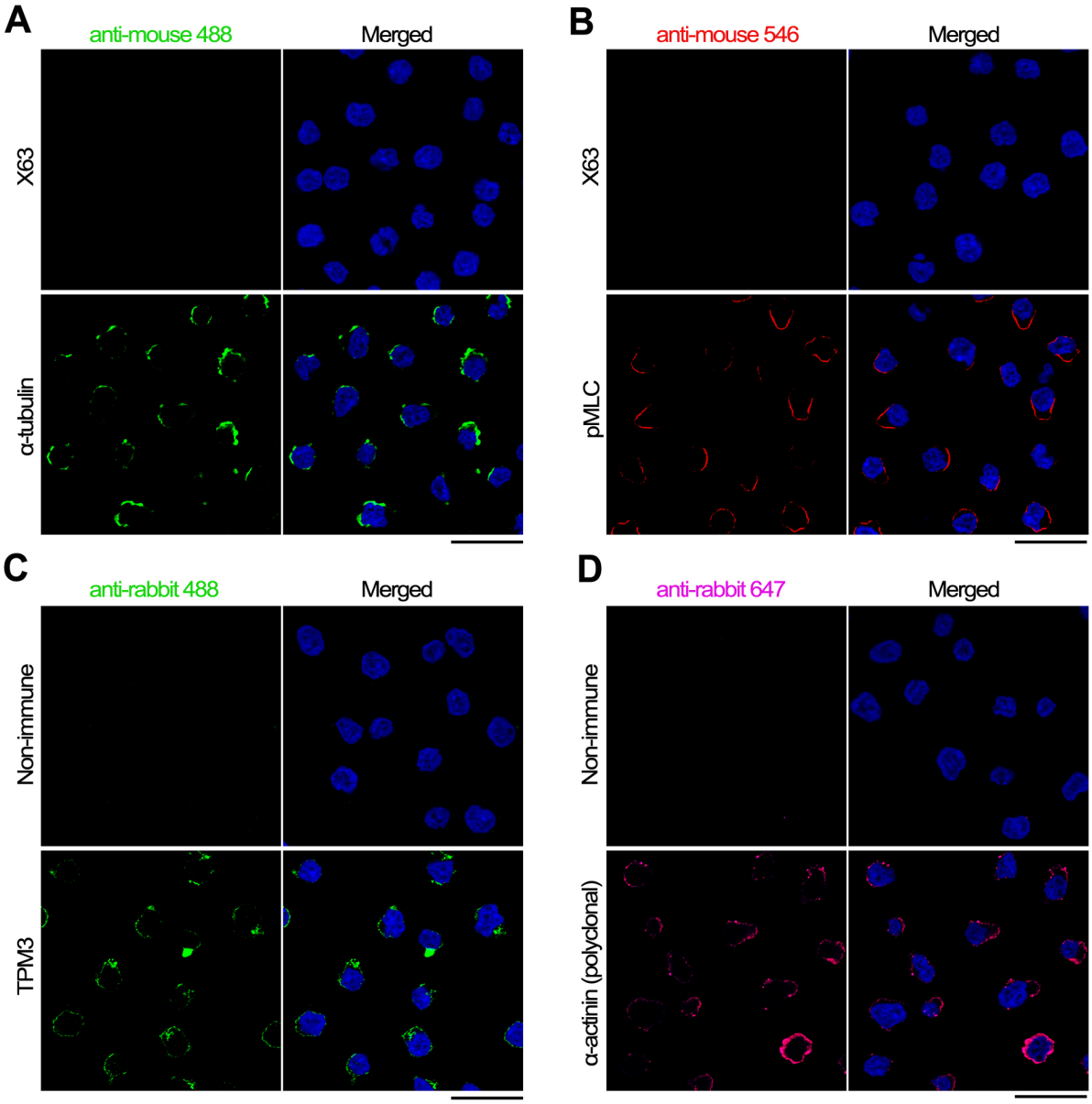

Supplementary Figure 10. Representative staining with non-specific antibodies used as negative control. Toledo cells were transduced with control shRNA, seeded on coverslips coated with 2 µg fibronectin, and stimulated with 10 ng/ml SDF1 for 15 min. Representative confocal microscopy images (1 section) of Toledo cells stained with DAPI and (**A**) anti-α-tubulin or the non-specific X63 mouse mAbs; (**B**) anti-pMLC or X63; (**C**) rabbit anti-TPM3 or a non-immune rabbit serum; and (**D**) rabbit anti-α-actinin or a non-immune rabbit serum. Scale bar, 10 µm.